Original Article

NLBK alleviates airway remodeling in COPD by inhibiting RXRA-mediated transcription of PLA2G2A

Teng Zhang¹, Fang Fang², Dan Wu², Guodong Wang²

¹Affiliated Mental Health Center & Hangzhou Seventh People's Hospital, Zhejiang University School of Medicine, Hangzhou, Zhejiang, P. R. China; ²Hangzhou TCM Hospital Affiliated to Zhejiang Chinese Medical University, Hangzhou, Zhejiang, P. R. China

Received November 7, 2024; Accepted July 5, 2025; Epub August 15, 2025; Published August 30, 2025

Abstract: Objectives: Nourishing lung benefiting kidney granule (NLBK) is used to treat chronic obstructive pulmonary disease (COPD). However, the molecular mechanism underlying its therapeutic effect is still unclear. In this study, we elucidated the molecular mechanism by which NLBK alleviates airway reorganization in COPD. Methods: We investigated the function of NLBK in regulating inflammatory reactions and endoplasmic reticulum stress (ERS) in mice with COPD. Through bioinformatics and network pharmacology analysis, we identified the main components and targets: Zhebeiresinol-nuclear receptors such as Retinol X receptor A (RXRA) and Phospholipase A2, group IIA (PLA2G2A). A rescue experiment was performed to confirm the relationship between Zhebeiresinol and PLA2G2A in alleviating COPD symptoms. Moreover, by conducting a series of experiments, we determined the transcriptional regulation of RXRA on PLA2G2A. Results: NLBK significantly inhibited cigarette smoke exposure-induced inflammatory response, lung function injury, and ERS in COPD mice Thebeiresinol acted as an active ingredient of NLBK, which was found to mitigate the inflammatory response, lung function injury, and ERS in COPD mice through the silencing of PLA2G2A, the specific target of NLBK. Zhebeiresinol repressed the phosphorylation of RXRA and entry into the nucleus, which efficiently suppressed the transcription of PLA2G2A. Conclusions: NLBK can alleviate airway remodeling in COPD through the RXRA-PLA2G2A axis, providing a new mechanistic basis for the clinical application of NLBK.

Keywords: Chronic obstructive pulmonary disease (COPD), yangfei yishen granule (NLBK), zhebeiresinol, phospholipase A2 group IIA (PLA2G2A), retinol X receptor A (RXRA)

Introduction

Chronic obstructive pulmonary disease (COPD) is a common, preventable, and treatable disease that has high morbidity and mortality rates worldwide [1]. There are more than 300 million COPD patients, with a prevalence rate of 11.7% [2]. COPD is characterized by persistent respiratory symptoms and airflow limitations resulting from airway and/or alveolar abnormalities and is closely associated with a chronic inflammatory response in the lungs to noxious gases or particles, which may further lead to respiratory failure [3, 4]. When the airway mucosa is exposed to infection, smoke, dust, and other factors, the local innate immunity of lung tissue is activated, releasing proinflammatory cytokines and chemokines to trigger the inflammatory response [5]. The number of T-lymphocytes and B-lymphocytes in the small airways and lung parenchyma is significantly increased, and the adaptive immune disorder mediated by these T-lymphocytes is an important reason for the progression of COPD [6, 7]. The main syndrome in the stable stage of COPD is a deficiency of lung and kidney qi [8, 9]. The control of inflammatory reactions is an important method for treating COPD. Nourishing the lungs and kidneys may treat COPD by regulating inflammation, immunity, and hypoxia tolerance, improving clinical symptoms, and improving the quality of life and lung function of patients [9]. Glucocorticoids and theophylline are mainly used to treat COPD [10, 11]. Although they help relieve symptoms, they have limited effects on controlling COPD progression because they do not effectively inhibit airway remodeling. Previous clinical trials have demonstrated the

efficacy of nourishing the lung benefiting kidney granules (NLBK) in treating COPD [12]. Treatment of patients with COPD with NLBK can improve the balance of inflammatory factors and prevent respiratory failure [13]. However, the molecular mechanism by which NLBK treats COPD remains unclear.

Endoplasmic reticulum stress (ERS)-related apoptosis is one of the pathogenic factors of COPD [14]. ERS is a key signal triggering tissue remodeling under pathological conditions and triggers tissue remodeling under such conditions [15, 16], Inflammatory responses, oxidative stress, calcium dysregulation, and other factors can contribute to the destruction of the oxidative environment of the endoplasmic reticulum (ER), leading to a massive accumulation of misfolded or unfolded proteins that further induce ERS [17, 18], When ERS occurs, cells activate the unfolded protein response (UPR) signaling pathways that reduce the rate of protein synthesis to relieve the ER burden and protect the cell [19]. However, when the UPR is out of control, and the ER induces apoptosis through transcription and caspase activation of the CCAAT/enhancer-binding protein (C/EBP) homolog, this promotes the secretion of mucin and hyaluronic acid in airway epithelial cells, the chemotaxis of inflammatory cells, and the imbalance of calcium homeostasis, leading to airway remodeling [20].

Pingchuan granules improve airway remodeling in mice by regulating ERS via the protein kinase R-like endoplasmic reticulum kinase signaling pathway [21]. Through bioinformatics analysis and network pharmacology, we found that NLBK, retinoid X receptor-alpha (RXRA), and secretory phospholipase A2IIA (PLA2G2A) may have regulatory relationships. PLA2G2A is an enzyme associated with acute respiratory distress syndrome (ARDS). Inflammatory factors promote the expression of PLA2G2A through transcription factors such as nuclear factor kappa-B (NF-кb) and the signal transducer and activator of transcription (STAT) family and amplify the inflammatory response in airway smooth muscle cells [22, 23]. Additionally, the compound roo-cough-zupak can protect lung function by inhibiting the expression of PLA2G2A in a mouse model of COPD [24]. RXRA is a member of the nuclear receptor ligand-dependent transcription factor family [25]. Moreover, RXRA regulates PLA2G2A to alleviate delirium in patients with COPD by affecting ERS and cell apoptosis [25]. Thus, the RXRA-PLA2G2A axis may help elucidate the molecular mechanism by which NLBK attenuates ERS.

In this study, we constructed a mouse model of COPD. We performed bioinformatics analysis and network pharmacological analysis to determine the potential mechanism: NLBK inhibited the inflammatory response, ERS, and airway remodeling damage by inhibiting the phosphorylation of RXRA, which in turn inhibited the transcription of PLA2G2A.

Methods

Cell culture and treatment

The cell line, 16 human bronchial epithelial (16HEB) cells (NO. MZ-1420; Ningbo Mingzhou Biotechnology Co., Ltd.) were cultured in DMEM supplemented with 10% fetal bovine serum (FBS) at 37°C. Next, 16HEB cells were seeded at a density of 1.5 × 10⁵ cells/mL on culture plates and incubated for 12 h. The cells were then incubated in an FBS-free medium for 3 h, followed by exposure to 10% cigarette smoke (CSE) for 24 h containing FBS. Then, the 16HBE cells were treated with NLBK (35 mg/mL; Jiangyin Tianjiang Pharmaceutical Co., Ltd.), zhebeiresinol (40 µg/mL; Invevo Chemical Technology (Guangzhou) Co., Ltd.), or water for 24 h. NLBK that met the standards of the Chinese Pharmacopoeia (2015 Edition) contained Rehmanniae Radix Praeparata (9 g), Schisandrae Chinensis Fructus (9 g), Platycodon Grandiforus (9 g), Figwort Root (9 g), Pseudostellariae Radix (9 g), Ophiopogon japonicus (9 g), Radix Rehmanniae (12 g), Trichosanthes Kirilowii Maxim (12 g), Hedysarum Multijugum Maxim (15 g), Lilii Bulbus (15 g), Mori Cortex (6 g), Fritillariae Thunbrgii Bulbus (6 g), Radix Glycyrrhizae (6 g). NLBK was put in water (1 L). All the components were extracted by boiling in 400 mL water for 1.5 h. Briefly, one cigarette was burned for 5 min and dissolved in 10 mL of PBS (pH 7.4) using a syringe. Then, the solution was filtered with 100% CSE solution.

COPD model

Initially, C57BL/6J wild-type mice were raised at the Animal Experimental Center of Zhejiang

University (SYXK (Zhejiang) 2022-0037). The animals were fed adaptively for one week before the experiment. The mice were randomly divided into the following groups: the control group (Ctrl group, n = 10), COPD group (n = 10), COPD + PBS group (n = 10), COPD + NLBKgroup (n = 10), COPD + Zhebeiresinol group (n = 10), COPD + Zhebeiresinol + shNC group (n = 10), and COPD + Zhebeiresinol + shPLA2G2A group (n = 10). The mice were infected twice a week by intranasal administration of 5 µg of AAV-shPLA2G2A or sh-NC (GenePharma) for two weeks. Two weeks after the infection, a COPD model was established [26]. The mice breathed normal air at the same time every day in a custom-made plastic smoke room (100 × 70 × 40 cm), and 0.2 mL of saline was instilled into each airway of the mice on the 1st and 28th days. COPD model mice were exposed to 20 cigarettes in a custom-made plastic smoke chamber twice a day for 30 min at intervals of 8 h for 50 days. When the mice experienced symptoms such as decreased activity, arched back, cough, increased nasal secretions, shallow breathing, wheezing, and highly paradoxical breathing in the chest and abdomen, we considered that the mouse model of COPD was successfully established. The NLBK-treated or zhebeiresinol-treated mice were gavaged with 2 mL of NLBK (4 g/kg) or 2 mL of zhebeiresinol (40 mg/kg) daily from the 29th day to the 50th day. The Ctrl group and CSE group were gavaged with 2.0 mL of water once a day. The mice were euthanized via the intraperitoneal injection of 200 mg/kg sodium pentobarbital.

Construction of the AAV and intratracheal administration

Using the AAV1 vector, the U6 promoter-driven shRNA expression system was established by OBiO Biotechnology (Shanghai) Co., Ltd. PLA2G2A shRNA was designed based on the shRNA sequence. Two selected target sequences of shRNA were inserted between the EcoRI and BamHI sites in a U6-CMV-EGFP/AAV vector. The PLA2G2A targets (sequence: shPLA2G2A: 5'-GAA ACA AGA CGA CCT ACA A-3'; shRXRA #1: 5'-GGC GAT ATG GCT GTG TCC CGG C-3'; shRXRA #2: 5'-GTG TTG TCA CCC TCC TTA TTT-3') were selected. A recombinant adenovirus without any shRNA sequence was included as a negative control (shNC). All constructs were verified via DNA sequencing, and all the viral vectors

were generated via triple plasmid cotransfection of human 293 cells. The recombinant virions were purified using column chromatography. Additionally, qPCR was performed to determine the viral titers. The AAV1-PLA2G2A-shRNA titer was confirmed to be 1.3 \times 10^{12} vector genomes (vg)/mL. The AAV1-PLA2G2A-shRNA titer (50 μ L) was intratracheally administered using the PenWu Device for Mouse (Bio Jane, Cat. No. BJ-PW-M, Shanghai).

Analysis of pulmonary function

The mice were anesthetized via an intraperitoneal injection of 70 mg/kg sodium pentobarbital. Then, they were placed in a body-tracing box and incubated. The respiratory rate (RI), forced expiratory volume (FEV) at 0.3 s, dynamic compliance (Cydn), inspiratory frequency (F), end-expiratory volume (EFP), minute volume (MV), and expiratory volume (EV) data were collected using the BUXCO non-invasive pulmonary function instrument system (SpirOx Pro, MEDITECH).

ELISA analysis

The levels of inflammatory cytokines, including interleukin (IL)-6 (RAB0309, Sigma-Aldrich), IL-13 (RAB0257, Sigma-Aldrich), IL-12 (RAB0255, Sigma-Aldrich), IL-10 (RAB0245, Sigma-Aldrich), IL-5 (RAB0304, Sigma-Aldrich), interferon (IFN)- γ (RAB0224, Sigma-Aldrich), IL-1 β (RAB0274, Sigma-Aldrich), and tumor necrosis factor (TNF)- α (RAB0477, Sigma-Aldrich), in mouse lungs were assessed via enzyme-linked immunosorbent assay (ELISA). Saline (1 mL) containing 5% FBS was slowly injected into the lungs of the mice through tracheal intubation. The bronchoalveolar lavage fluid (BALF) was centrifuged, and the supernatant was collected following the instructions provided with the kit.

HE staining

The lung tissue was fixed in 4% PFA and embedded in paraffin. The lung tissue slices (5 μ m) were deparaffinized and rehydrated. Then, the slices were stained with hematoxylin solution for 5 min. The stained slices were soaked in HCl-ethanol five times and rinsed with distilled water. After the slices were stained with eosin for 3 min, they were washed with $\rm H_2O$, dehydrated with graded alcohol, and cleaned with xylene. Finally, the slices were mounted with

neutral balsam and observed under a light microscope.

Detection of inflammatory cells

The cells from the BALF were stained with a combination of anti-mouse fluorochrome-conjugated mAbs to quantify the number of inflammatory cells via flow cytometry.

Western blotting

Protein expression was determined via Western blotting. The cells or tissues were lysed in a lysis buffer supplemented with a protease inhibitor cocktail. Protein (15 µg) was resolved by sodium dodecyl sulfate-polyacrylamide gel electrophoresis and transferred to polyvinylidene difluoride membranes for immunoblotting. The membranes were blocked in blocking buffer (5% skim milk in TBS) for 1 h at room temperature, followed by incubation with primary antibodies overnight at 4°C. The primary antibodies used were as follows: p-protein kinase RNA-like ER kinase (p-PERK) (1:1000, ab192591, Abcam), PERK (1:1000, ab229912, Abcam), p-inositol-requiring enzyme 1 alpha $(p-IRE1\alpha)$ (1:1000, ab243665, Abcam), IRE1 α (1:1000, ab37073, Abcam), activating transcription factor 4 (ATF4) (1:1000, ab270980, Abcam), ATF6 (1:1000, ab122897, Abcam), matrix metalloproteinase 9 (MMP9) (1:1000, ab76003, Abcam), fibronectin (1:1000, ab24-13, Abcam), vimentin (1:1000, ab20346, Abcam), and E-cadherin (1:1000, ab231303, Abcam). The membranes were subsequently incubated with HRP-conjugated goat antimouse or anti-rabbit IgG secondary antibodies (1:5,000; 31430 and 31460; Thermo) for 1 h at room temperature. The protein bands were visualized using enhanced chemiluminescence (ECL) kits. The images were scanned with a ChemiDoc Touch imaging system (Bio-Rad) and analyzed with ImageJ.

Quantitative real-time PCR (qPCR)

Quantitative real-time PCR (qPCR) was performed to assess the mRNA levels. Total RNA was extracted using TRIzol buffer and reverse-transcribed into cDNA using 4× Reverse Transcription Master Mix. The 2× SYBR Green qPCR Master Mix was used to perform qPCR following this procedure: denaturation at 95°C for 50 s, denaturation at 95°C for 5 s, anneal-

ing at 60°C and extension for 50 s, and 40 cycles were performed. Glyceraldehyde-3-phosphate dehydrogenase (GAPDH) was used as the internal parameter, and the relative expression of the detected genes was calculated using the 2-AACT method [27]. The primers used were as follows: PLA2G2A-Forward: 5'-CGG CAC CAA ATT TCT GAG CTA-3'; PLA2G2A-Reverse: 5'-AGC AGC CTT ATC GCA TTC AC-3'; GAPDH-Forward: 5'-CAC CCA CTC TTC CAC CTT C-3'; GAPDH-Reverse: 5'-CCT GTT GCT GTA GCC AAA TTC-3'.

ChIP-quantitative polymerase chain reaction (ChIP-qPCR)

For the ChIP-quantitative polymerase chain reaction (ChIP-qPCR), the cells were incubated with 1% PFA and glycine to terminate cross-linking. Fragments of size 200-1000 bp were obtained via ultrasonic fragmentation. The RXRA antibody-antigen complex or p-RXRA antibody-antigen complex was precipitated with protein A gel magnetic beads. After elution and washing, NaCl was added to the sample so that it could crosslink. RNaseA and proteinase K were then added for 2 h. DNA fragments were recovered for qPCR.

Dual-luciferase reporter assay

A dual-luciferase reporter assay was conducted following the method described in another study [28]. The recombinant plasmids containing the PLA2G2A promoter (wild-type and mutant type) and RXRA-shRNA were constructed and cotransfected into 293T cells; the empty vector was used as a control. Zhebeiresinol was added to the cells, and PBS was used as the control. After 48 h, the cells were collected, and the luciferase activity was detected with a dual luciferase detection kit (11402ES60, Yeasen).

Liquid chromatography-tandem MS analysis

Liquid chromatography-tandem mass spectrometry (LC-MS/MS) analysis was conducted to measure the active compounds of NLBK. The targeted analysis of NLBK was performed using an Agilent QTOF 6550 mass spectrometer equipped with an electrospray ionization source and an Agilent 1290 UPLC liquid chromatograph. An ABEH C18 2.1 × 100 mm, 1.7 µm column (Waters) was used with a flow rate of 0.3

mL/min and a sample volume of 5 μ L. The mass spectrometric analysis was conducted in the positive ion mode, with the sheath gas temperature and flow rate set at 350°C and 12 L/min, respectively. The voltage settings were 4000 V for the ESI+ mode and 3200 V for the ESI- mode.

Bioinformatics analysis and network pharmacological analysis

The data were obtained from the Gene Expression Omnibus (GEO) database (GSE38-974 and GSE76925): https://www.ncbi.nlm. nih.gov/geo/. The thresholds of |log2 fold change (FC)| > 1 and P < 0.05 were used to screen the differentially expressed genes (DEGs). Differential analysis was performed to identify highly DEGs. The active components of NLBK were obtained from the Traditional Chinese Medicine Systems Pharmacology (TCMSP) database (https://old.tcmsp-e.com/ tcmsp.php) and the Herb database (http:// HERB.ac.cn/). The bioavailability and pharmacodynamics of the active compounds were ≥ 30% and \geq 0.18, respectively. The target genes were obtained from the UniProt database (https://www.UNIPROT.org/). Next, the genes common to the drug-related target genes and the GEO differential genes were selected as candidate genes. Finally, to elucidate the potential molecular mechanisms of the candidate genes, the hTFtarget database (http://bioinfo.life.hust.edu.cn/hTFtarget#!/download) and the ChIPBase v3.0 database (https://rnasysu.com/chipbase3/index.php) were used to find common transcription factors and identify the corresponding drug targets for these transcription factors.

Statistical analysis

The data were presented as the mean \pm standard deviation and analyzed by conducting two-tailed Student's t-tests. The Statistical Package for the Social Sciences (SPSS) program (version 24.0, SPSS Inc., Chicago, IL) was used for statistical analysis. Two-tailed paired or unpaired Student's t-tests were run for two independent samples. Analysis of variance was performed to determine differences among three or more groups. All differences among and between groups were considered to be statistically significant at P < 0.05.

Results

NLBK regulated airway remodeling by inhibiting inflammation and ERS in COPD mice

To examine the effects of NLBK on COPD, a mouse model of COPD was constructed. Analysis of the HE-stained samples revealed a significant increase in inflammatory cell infiltration, goblet cell proliferation, and thickening of the columnar epithelial layer in the COPD groups compared to that in the Ctrl group. NLBK treatment reduced the inflammatory reaction (Figure 1A). We also determined the levels of inflammatory cytokines in the serum. Compared to the mice in the Ctrl group, the mice in the COPD group presented significantly higher levels of TNF- α (P < 0.05), while treatment with NLBK significantly impaired the CSEmediated increase in TNF- α (**Figure 1B**). The ELISA results showed that the changes in IL-1β were similar to those of TNF- α (**Figure 1C**). The levels of IL-5 and IL-10 increased substantially in CSE-treated mice but were attenuated by NLBK intervention (P < 0.05) (Figure 1D and 1E). Functional assays revealed that the CSEinduced increase in the IL-13 level was partially reversed after NLBK intervention (P < 0.05; Figure 1F). In contrast to the Ctrl group, there was a significant decrease in IL-12 levels in the COPD group (P < 0.05), but NLBK reversed the decrease in IL-12 caused by CSE (P < 0.05) (Figure 1G). On the other hand, lower levels of IFN-y were observed in the mice with COPD, while NLBK significantly increased the levels of IFN-y in these mice (P < 0.05; **Figure 1H**). After CSE, the number of total cells increased significantly (P < 0.05). NLBK played an important role in preventing the increase in the number of total cells compared to that in the COPD group (P < 0.05; **Figure 2A**). In the COPD group, the number of macrophages (Figure 2B), eosinophils (Figure 2C), and neutrophils (Figure 2D) increased significantly (P < 0.05), whereas NLBK significantly reversed the CSE-mediated increase in the number of macrophages, eosinophils, and neutrophils (P < 0.05). Moreover, we confirmed that the changes in CD4+ and CD8⁺ T lymphocytes were similar to those in macrophages (Figure 2E and 2F). These findings strongly suggested that NLBK intervention helps alleviate the inflammatory state of COPD patients.

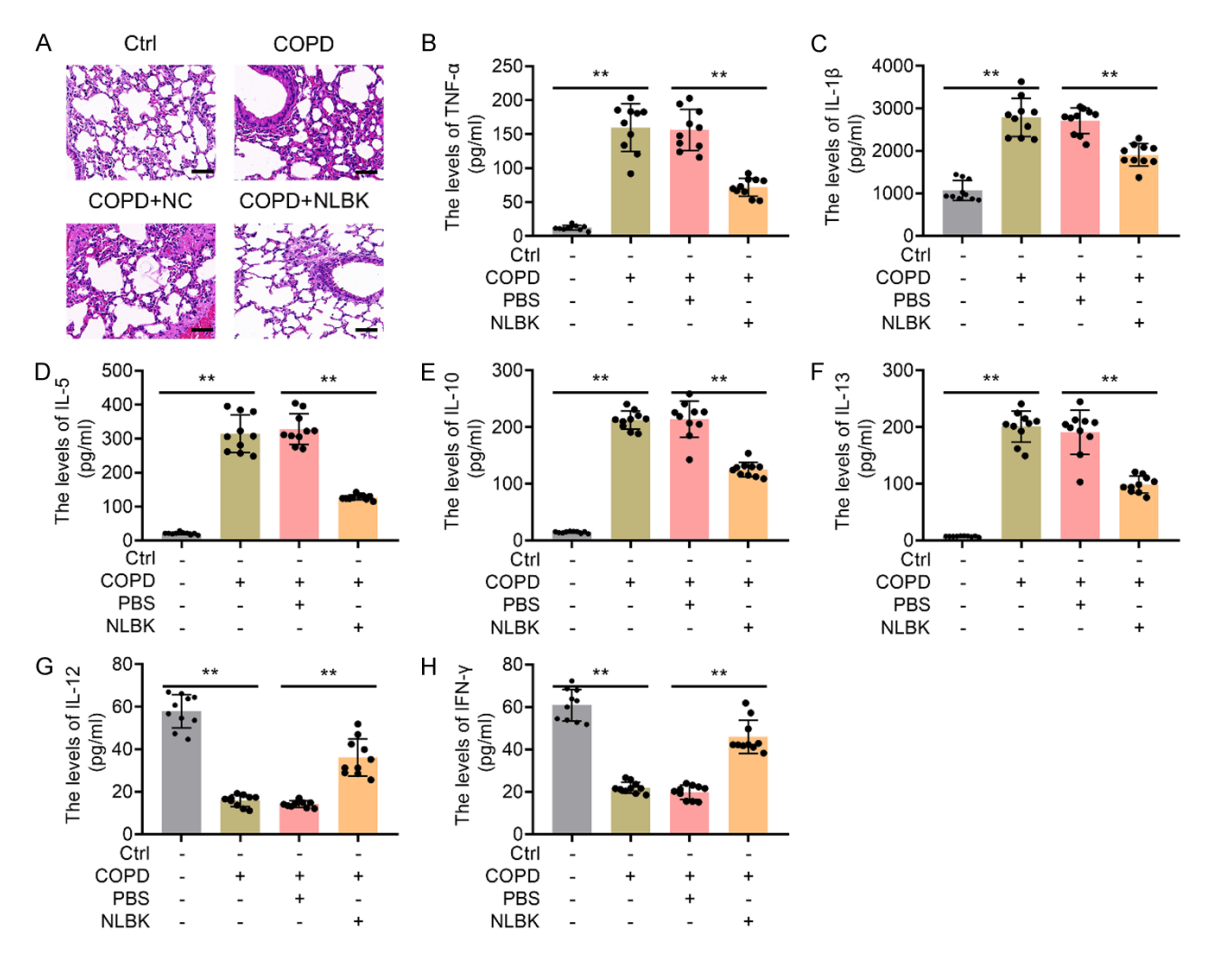


Figure 1. NLBK significantly rescued the CSE-mediated increase in inflammatory cytokines in COPD mice. (A) Representative images of HE-stained lung tissue from COPD mice receiving NLBK treatment (scale bar = 100 μm). (B-H) ELISA was performed to measure the levels of inflammatory cytokines in COPD mice receiving NLBK treatment. The levels of (B) TNF- α , (C) IL-13, (D) IL-12, (E) IL-10, (F) IL-5, (G) IFN- γ , and (H) IL-1 β ; **P < 0.01.

We also investigated whether NLBK can alleviate the damage to pulmonary function induced by CSE. CSE significantly increased the RI (P < 0.05), and these effects were partially reversed by NLBK intervention (P < 0.05; Figure 3A). The decrease in the FEVO.3/FVC ratio in COPD mice was inhibited by NLBK intervention (P < 0.05; Figure 3B). Additionally, the decrease in Cydn levels was partially reversed by NLBK in COPD mice (P < 0.05; Figure 3C). Our results also revealed that NLBK had a greater ability to ameliorate the CSE-mediated promotion of F and EEP (P < 0.05; Figure 3D and 3E). CSE reduced the levels of EV and MV compared to their levels in the Ctrl group, whereas NLBK treatment inhibited the reduction in the levels of EV and MV caused by CSE (Figure 3F and 3G).

Next, the levels of ERS-related proteins were determined via Western blotting analysis. As shown in Figure 4A, BIP was expressed more abundantly in the COPD group than in the Ctrl group, which was inhibited by NLBK treatment. Similarly, the increase in the levels of p-PERK/PERK and p-IRE1α/IRE1α induced by CSE was also inhibited by NLBK. The level of expression of ATF4 and ATF6 increased substantially after CSE, whereas NLBK abrogated the effects of CSE on ATF4 and ATF6 expression. We also investigated the expression of airway remodeling-related proteins (Figure 4B). The expression levels of MMP9, fibronectin, and vimentin increased significantly in COPD mice. However, NLBK weakened the effect of CSE on these proteins. The expression levels of E-cadherin were opposite those of MMP9 and other proteins.

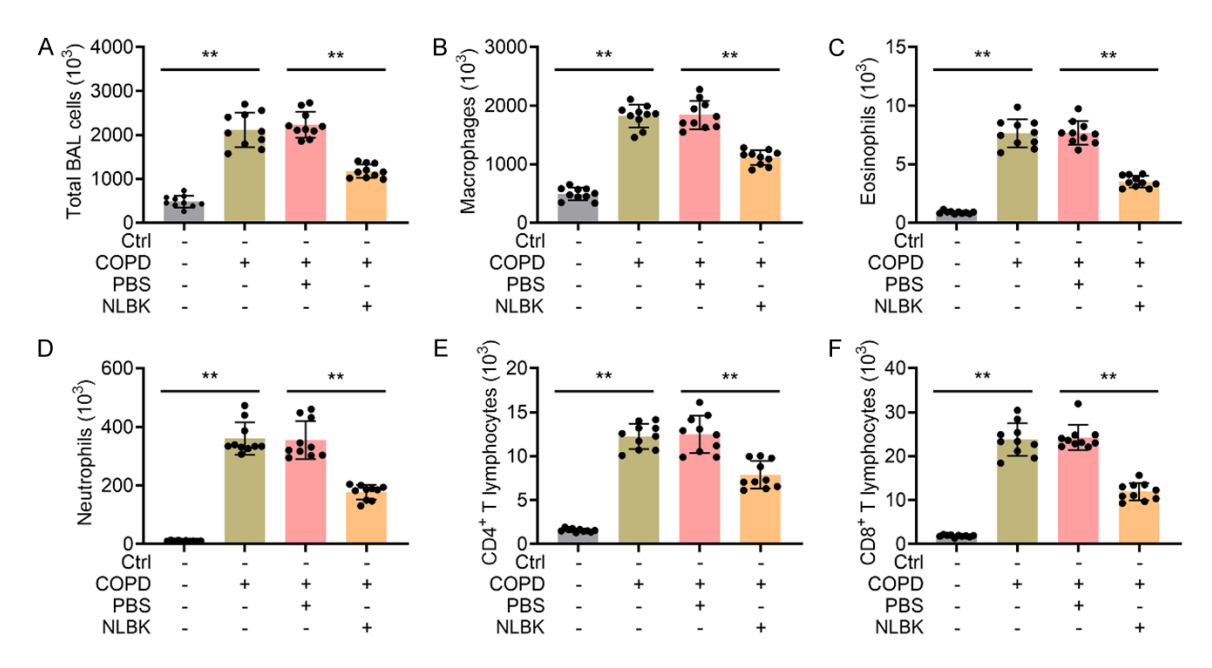


Figure 2. NLBK significantly rescued the CSE-mediated increase in inflammatory cells in the BALF. The number of total BALF cells (A), macrophages (B), eosinophils (C), neutrophils (D), CD4⁺ T lymphocytes (E), and CD8⁺ T lymphocytes (F) were determined using cytospin; **P < 0.01.

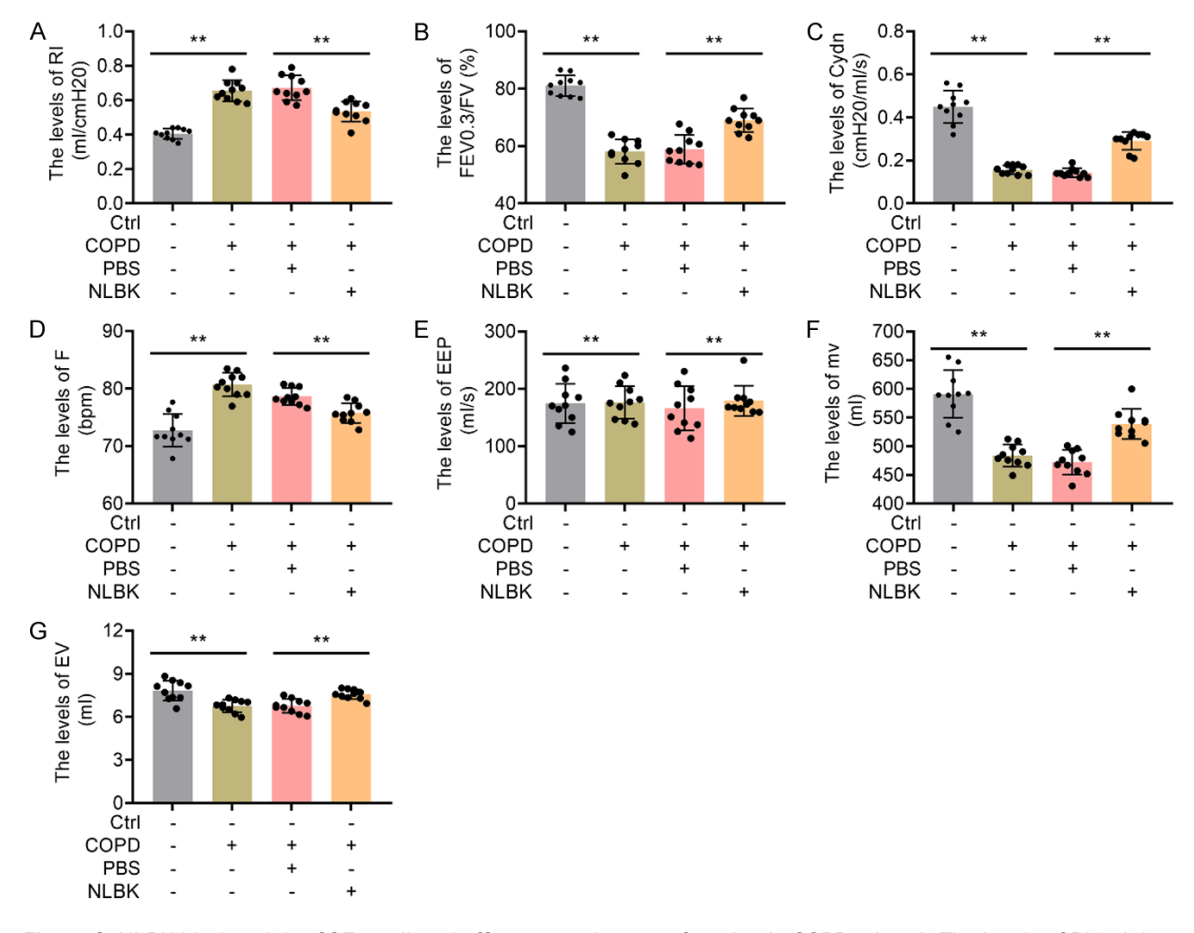


Figure 3. NLBK hindered the CSE-mediated effects on pulmonary function in COPD mice. A. The levels of RI (mL/cm H_2O). B. The values of FEV0.3/FVC (%). C. Cydn levels (cm $H_2O/mL/s$). D. The levels of F (bpm). E. The levels of EEP (mL/s). F. The levels of MV (mL). G. EV levels (mL); **P < 0.01.

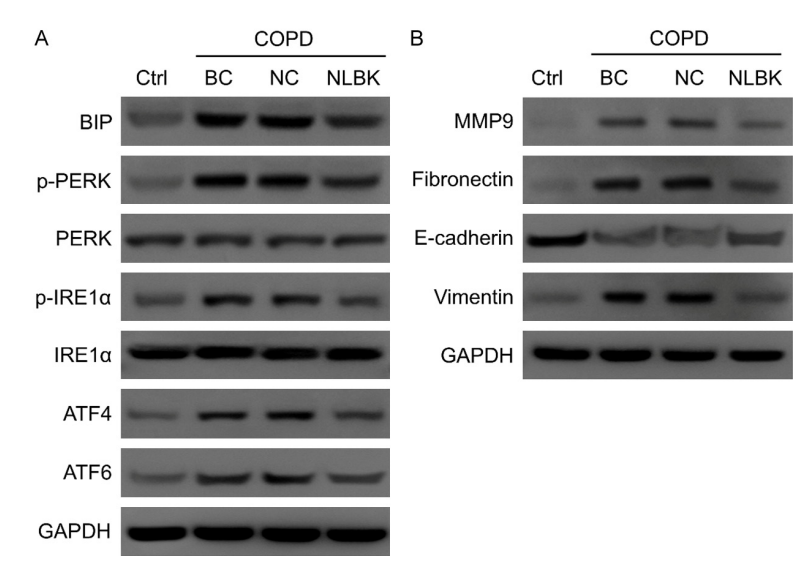


Figure 4. NLBK reversed the effects of CSE on ERS-related and airway remodeling-related proteins in COPD mice. A. Western blotting was performed to detect the expression levels of ERS-related proteins. B. Expression levels of airway remodeling-related proteins.

The targets of NLBK were identified via network pharmacology and mass spectrometry analysis

We investigated the mechanisms by which NLBK alleviated airway remodeling in COPD model mice. Bioinformatics analysis was performed to identify the hub genes related to COPD using data from the GEO. A diagram of the bioinformatics analysis and network pharmacology analysis procedures is illustrated in Figure 5A. The results revealed 128 DEGs, among which 30 were upregulated and 98 were downregulated (Figure 5B). Hierarchical clustering revealed the expression patterns of the DEGs between the COPD and control samples (Figure 5C). The regulatory roles were predicted by analyzing the functions of the 128 DEGs through GO analysis (Figure 5D). GO annotations (P < 0.05) involving the top five pathways included multiple biological processes, cellular components, and molecular functions. Next, we evaluated the targets of NLBK through network pharmacology. We obtained 153 active components and 733 targets of NLBK from the Chinese systems pharmacology database, analysis platform, and herbal group identification database (Supplementary Figure 1). A PPI network was constructed to illustrate the correlations between targets (Supplementary Figure 2). We subsequently performed mass spectrometry analysis and identified 176 NLBK compounds, including boschnialactone, watterose E, Gomphrenin III, miserotoxin, adenosine, and zhebeiresinol (Supplementary Files). Similar to the network pharmacology results, the qualitative mass spectrometry results revealed that zhebeiresinol (CAS: 151636-98-5) was also a compound target (Figure 5E and 5F).

Zhebeiresinol alleviated the inflammatory response and ERS through PLA2G2A

We investigated the downstream targets and regulatory mechanisms of NLBK by conducting rescue experiments. The Venn analysis revealed eight regulatory targets in

both COPD disease genes and NLBK-targeted genes, including BCHE, CCL19, SPP1, MMP9, HTR2B, PLA2G4A, CXCL13, and PLA2G2A (Figure 6A). Then, we performed a rescue experiment by knocking down PLA2G2A using short hairpin RNA (shRNA) (shPLA2G2A) and treating the cells with zhebeiresinol. Zhebeiresinol decreased the expression of PLA2G2A in COPD mice (Figure 6B). HE staining revealed that compared to those in the Ctrl group, a greater number of inflammatory cells infiltrated the lung tissue of the mice with COPD. However, zhebeiresinol intervention decreased the inflammatory state in COPD model mice. Knocking down PLA2G2A significantly inhibited the inflammatory state in COPD mice (Figure 6C). Then, the levels of inflammatory cytokines were measured. The ELISA results revealed that zhebeiresinol reversed the CSE-induced increase in TNF- α levels (P < 0.05). Silencing PLA2G2A further promoted the ability of zhebeiresinol to reduce TNF- α levels (P < 0.05; Figure 6D). Zhebeiresinol intervention decreased IL-1ß levels, and knocking down PLA2G2A after zhebeiresinol intervention further reduced IL-1 β levels (P < 0.05; **Figure 6E**). Moreover, the levels of IL-5. IL-10. and IL-13 were similar to those of IL-1ß (Figure 6F-H). Our results also revealed that zhebeiresinol intervention effectively alleviated the decrease in IL-12 levels in COPD mice. Moreover, knocking down PLA2G2A after zhebeiresinol intervention had a stronger

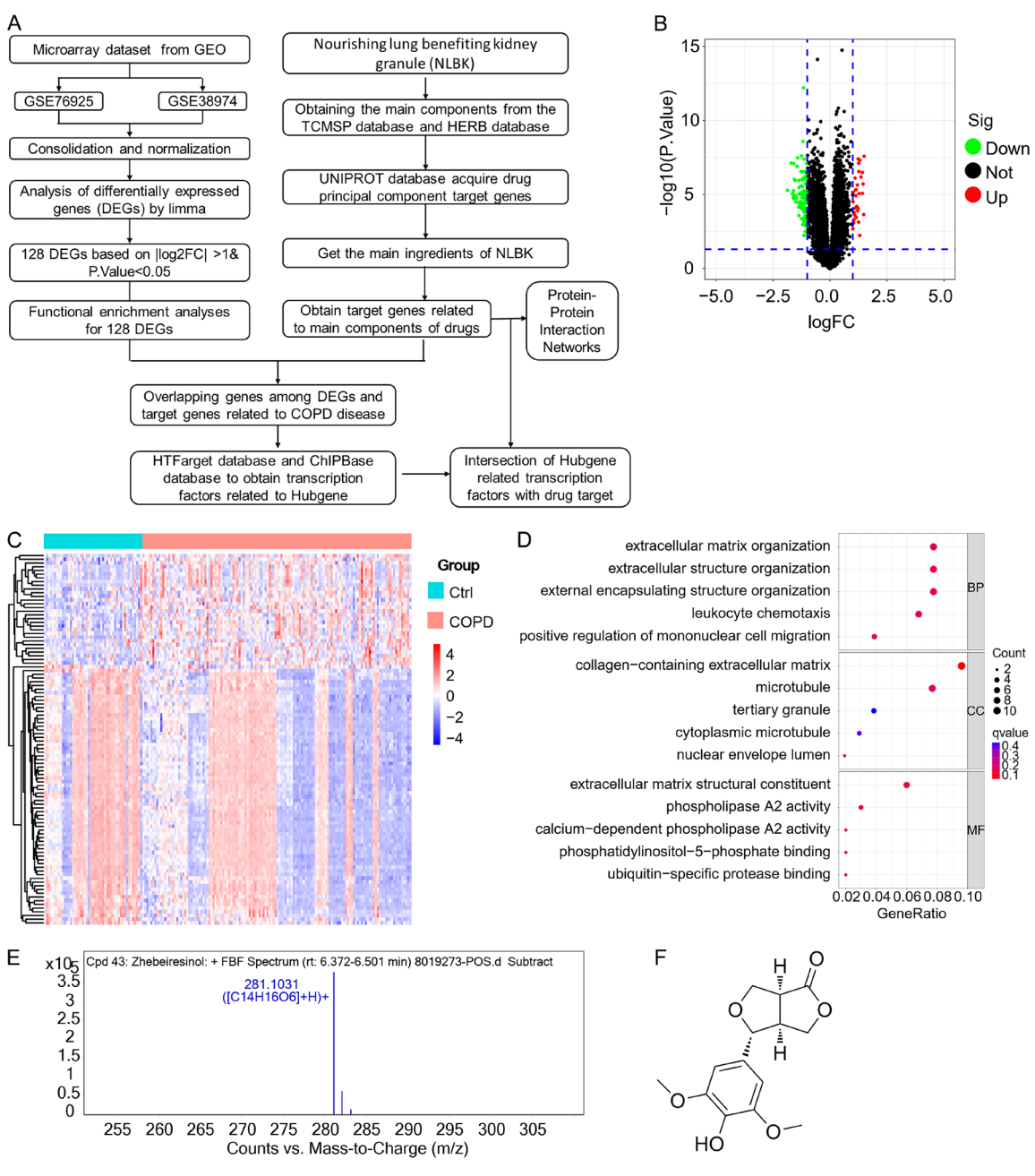
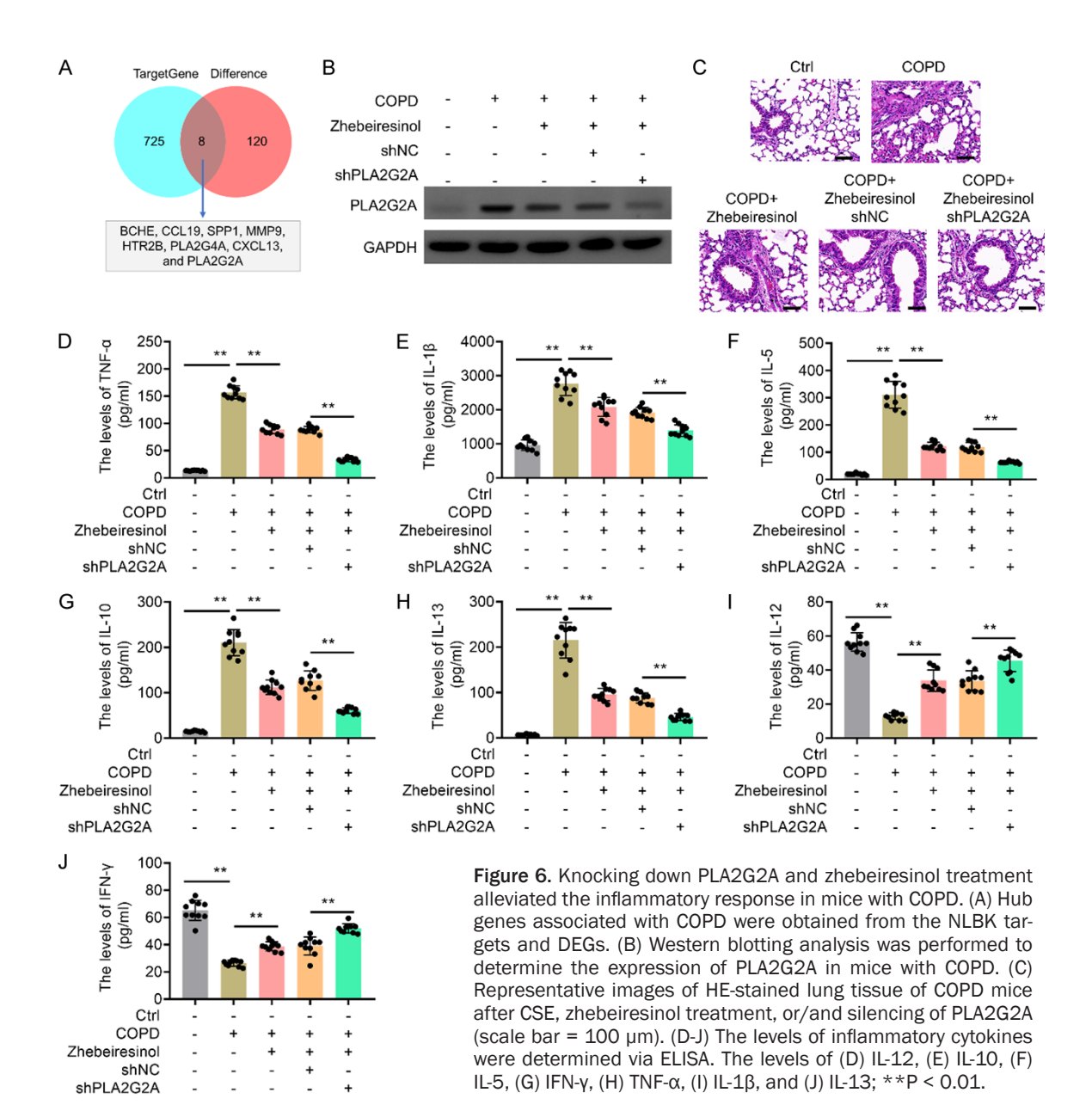


Figure 5. Identification of effective targets and active ingredients. A. The diagram shows the procedure for bioinformatics analysis and network pharmacology analysis. B. Volcano plot of the upregulated and downregulated DEGs in COPD patients. C. The heatmaps show the distribution of DEGs. D. GO annotations included multiple biological processes, cellular components, and molecular functions. E. The qualitative compound report was obtained via mass spectrometry. F. The structure of zhebeiresinol is shown.

promoting effect on the IL-12 level (P < 0.05; **Figure 6I**). Additionally, there was a dramatic decrease in IFN- γ levels in COPD mice following zhebeiresinol intervention. After zhebeiresinol intervention, the levels of IFN- γ increased considerably when PLA2G2A expression was inhibited in COPD mice (P < 0.05; **Figure 6J**). In BAL fluid, CSE significantly increased the number of

total cells, macrophages, eosinophils, and neutrophils; however, zhebeiresinol intervention significantly impaired the CSE-mediated increase in the number of these cells. Knocking down PLA2G2A further promoted the contribution of zhebeiresinol to decreasing the number of these cells (P < 0.05; Figure 7A-D). Additionally, zhebeiresinol intervention attenuated



the increase in the number of CD4 $^{+}$ and CD8 $^{+}$ T lymphocytes induced by CSE, whereas shPLA-2G2A transfection partially increased the activity of zhebeiresinol (P < 0.05; **Figure 7E** and **7F**).

For pulmonary function analysis, zhebeiresinol intervention inhibited the increase in the RI in the COPD mice (P < 0.05). The RI was further inhibited in the COPD mice in which PLA2G2A was knocked down (P < 0.05; Figure 8A). As shown in Figure 8B, the decrease in the FEV0.3/FVC in COPD mice was partially inhibited by zhebeiresinol intervention; silencing PLA2G2A increased the ability of zhebeiresi-

nol to increase the FEV0.3/FVC (P < 0.05). Zhebeiresinol intervention increased Cydn levels in COPD mice; PLA2G2A knockdown significantly enhanced the beneficial effects of zhebeiresinol on Cydn (P < 0.05) (Figure 8C). Pulmonary function analysis confirmed that zhebeiresinol intervention increased F levels and decreased MV levels; these benefits of zhebeiresinol were associated with silencing PLA2G2A (Figure 8D and 8E). Zhebeiresinol and PLA2G2A significantly affected EEP and EV (Figure 8F and 8G).

We also investigated the regulatory role of zhebeiresinol and PLA2G2A in ERS. The results of

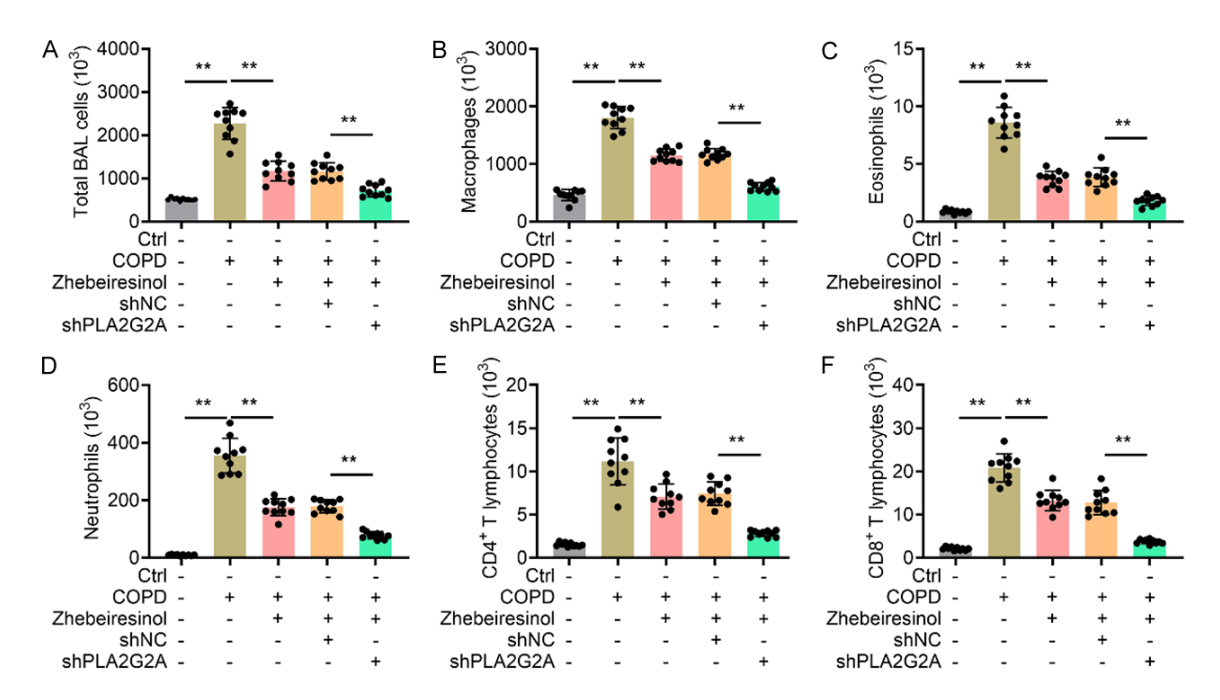
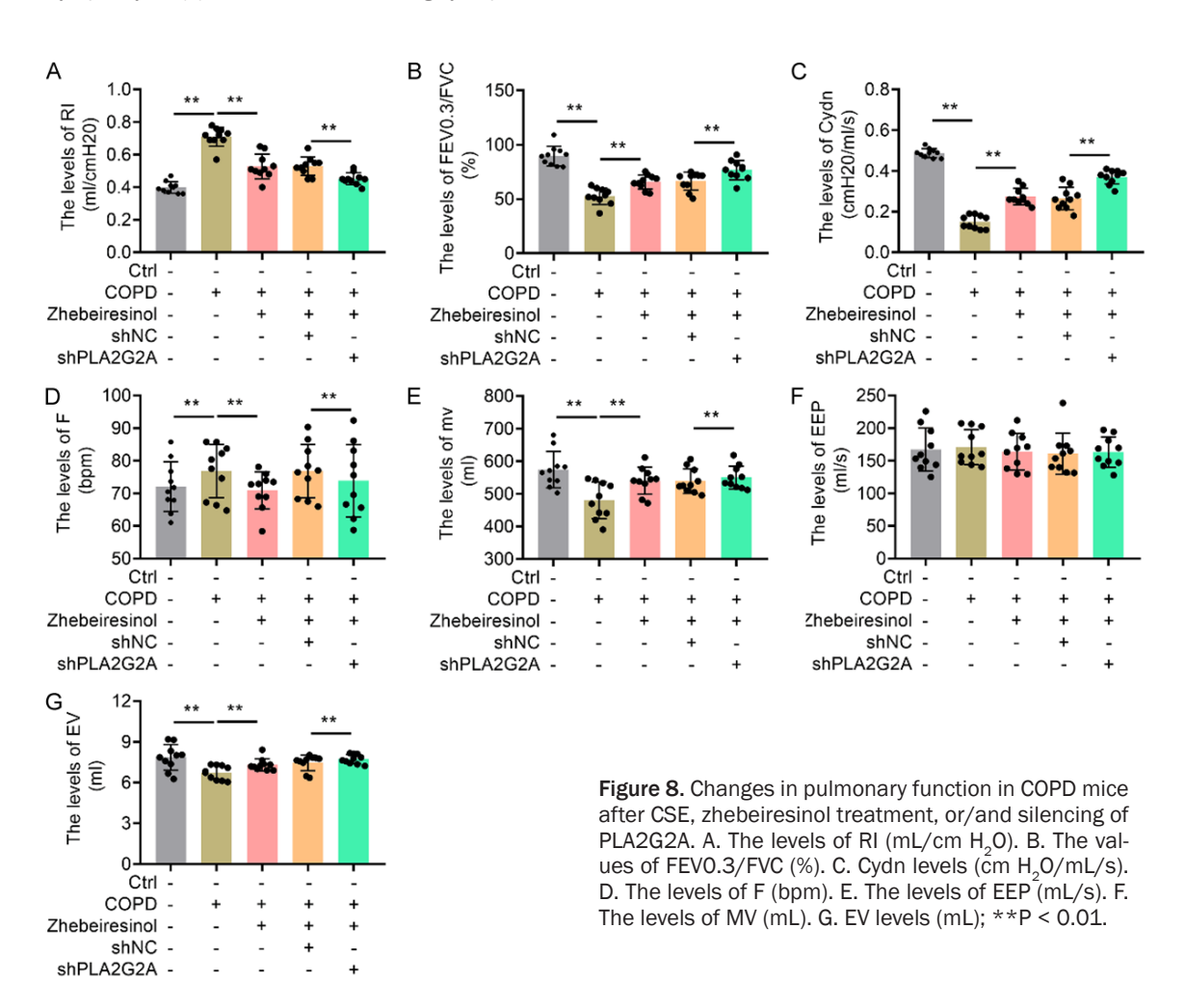


Figure 7. Knocking down PLA2G2A and zhebeiresinol treatment alleviated inflammatory cells in COPD mice. The number of total BALF cells (A), macrophages (B), eosinophils (C), neutrophils (D), CD4⁺ T lymphocytes (E), and CD8⁺ T lymphocytes (F) were determined using cytospin; **P < 0.01.



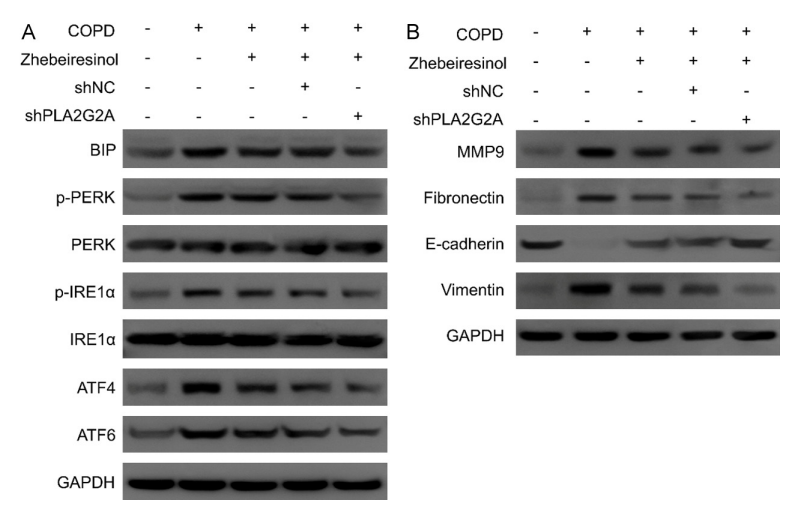


Figure 9. The expression levels of ERS-related and airway remodeling-related proteins in COPD mice after CSE, zhebeiresinol treatment, or/and silencing of PLA2G2A. A. The expression levels of ERS-related proteins were determined via Western blotting analysis. B. The expression levels of airway remodeling-related proteins were determined via Western blotting analysis.

Western blotting assays revealed that the expression levels of BIP were significantly reduced in COPD mice following zhebeiresinol intervention. Subsequently, silencing PLA2G2A resulted in a greater reduction in BIP expression. Moreover, the levels of p-PERK/PERK and p-IRE1 α /IRE1 α were similar to those of BIP. The increased expression of ATF4 and ATF6 was effectively inhibited by zhebeiresinol intervention in COPD mice, while the expression of ATF4 and ATF6 in the Zhebeiresinol + shPLA2G2A group was significantly lower than that in the Zhebeiresinol group (Figure 9A). Moreover, zhebeiresinol significantly rescued the increased expression of MMP9, fibronectin, and vimentin induced by CSE. However, knocking down PLA2G2A further decreased the expression of MMP9, fibronectin, and vimentin in the presence of zhebeiresinol. In contrast, zhebeiresinol significantly impaired the CSE-mediated reduction in E-cadherin in mice with COPD, whereas knocking down PLA2G2A resulted in a more significant impairment of zhebeiresinol (Figure 9B).

Zhebeiresinol regulated PLA2G2A transcription by inhibiting RXRA

We elucidated the mechanisms underlying circPTPRA regulation of IGF2BP1 function. A total of 35 transcription factors encoding PLA2G2A were obtained, including eight NLBK regulatory targets (ESR1, CREB1, AR, STAT3, STAT1, RXRA, PPARG, and JUN) (Figure 10A and 10B). The molecular docking results revealed that zhebeiresinol interacted with RXRA (Figure 10C). results of Western blotting assays revealed that NLBK intervention partially reversed the promoting effects of CSE on p-RXRA/RXRA (Figure 10D). We subsequently performed a nuclear-cytoplasmic separation experiment, and the results revealed that NLBK intervention significantly inhibited RXRA from entering the nucleus (Figure 10E). Additionally, zhebeiresinol intervention also significantly reduced p-RXRA/RXRA levels

and inhibited RXRA entry into the nucleus (Figure 10F and 10G). Moreover, knocking down RXRA effectively inhibited the expression of PLA2G2A (Figure 10H). A similar result was found for the mRNA levels of PLA2G2A (Figure 10I).

Next, we assessed whether RXRA regulated the expression of PLA2G2A. The DNA binding motif of RXRA was obtained using the JASPAR database (Figure 11A). Then, the prediction of binding sites with the PLA2G2A promoter was performed. Two binding sequences exist between RXRA and the PLA2G2A promoter, including between 1052 and 1069 and between 241 and 227 (Figure 11B). The results of the ChIP assay confirmed that RXRA has a strong affinity for the promoter region of PLA2G2A (Figure 11C and 11D). To investigate whether RXRA directly transcriptionally regulates the expression of PLA2G2A, luciferase assays were conducted, which revealed that RXRA induced the promoter activity of PLA2G2A in 293T cells transfected with the full promoter region of PLA2G2A. Compared to the full-length promoter construct, the P1 mutant (not containing the E2 RXRA binding site) did not exhibit a reduction in promoter activity after transfection of the RXRA knockdown plasmid (Figure 11E); this phenomenon was also observed in the P2 mutant (not containing the E1 RXRA binding site) (Figure 11F). These results indicated that

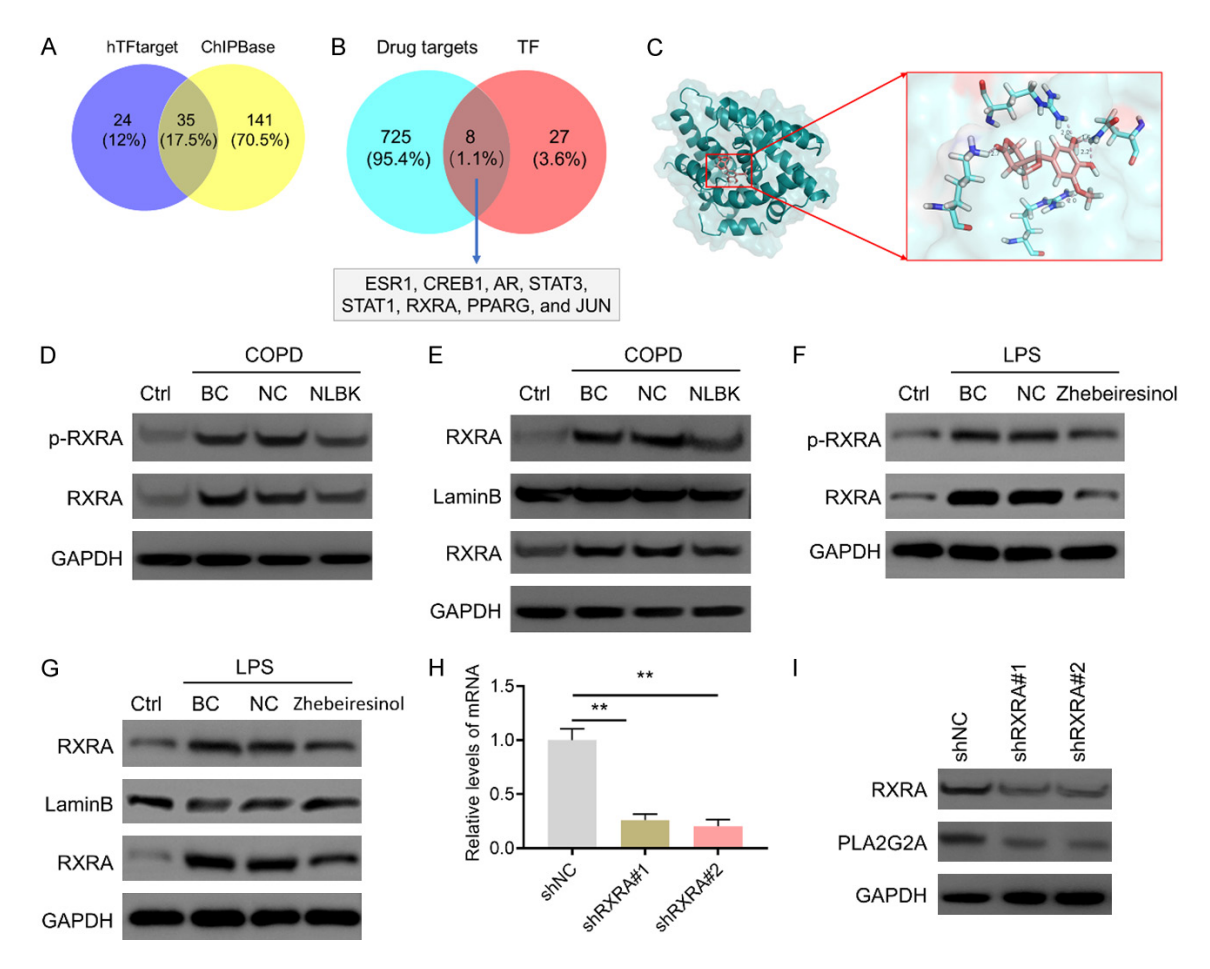


Figure 10. Zhebeiresinol inhibited the phosphorylation and nuclear entry of RXRA, a transcription factor of PLA2G2A. A. The transcription factors of PLA2G2A were identified using the hTFtarget database and ChIPBase v3.0. B. The common factors were determined using the transcription factors of the PLA2G2A and NLBK targets. C. The combination of zhebeiresinol and RXRA was predicted. D. The phosphorylation levels of RXRA were evaluated in the COPD model via Western blotting analysis. E. The expression of RXRA in the nucleus and cytoplasm was investigated in a COPD model via Western blotting analysis. Lamin B and GAPDH were used as loading controls. F. The phosphorylation levels of RXRA were evaluated via Western blotting after zhebeiresinol treatment. G. The expression of RXRA in the nucleus and cytoplasm was investigated after zhebeiresinol treatment. Lamin B and GAPDH were used as loading controls. H. The expression levels of PLA2G2A were assessed after RXRA was knocked down. I. The mRNA levels of PLA2G2A were determined after RXRA was knocked down; **P < 0.01.

the RXRA binding site in the promoter region of PLA2G2A is located at the E1 binding site (-241 bp to -227 bp) and the E2 binding site (-1069 bp to -1052 bp). Zhebeiresinol treatment also significantly decreased relative luciferase activity, whereas the P1 mutation (not containing the E2 RXRA binding site) eliminated the effect of RXRA on PLA2G2A transcription activity (**Figure 11G**). Zhebeiresinol treatment had a similar effect on the P2 mutant (**Figure 11H**). These results indicated that the RXRA binding site in the promoter region of PLA2G2A is located at the E1 binding site (-241 bp to -227 bp) and the E2 binding site (-1069 bp to -1052 bp).

Discussion

Chronic obstructive pulmonary disease (COPD) is a type of chronic respiratory disease that is not completely reversible and is progressive [29]. It can be effectively prevented and actively treated, and its pathophysiological characteristics include chronic inflammatory changes in the airway, lung parenchyma, and pulmonary vessels, which continue to develop. Chronic airway inflammation plays a key role in the development of COPD [30]. Substances, such as cigarettes, can stimulate airway cells to release inflammatory cytokines and lead to airway

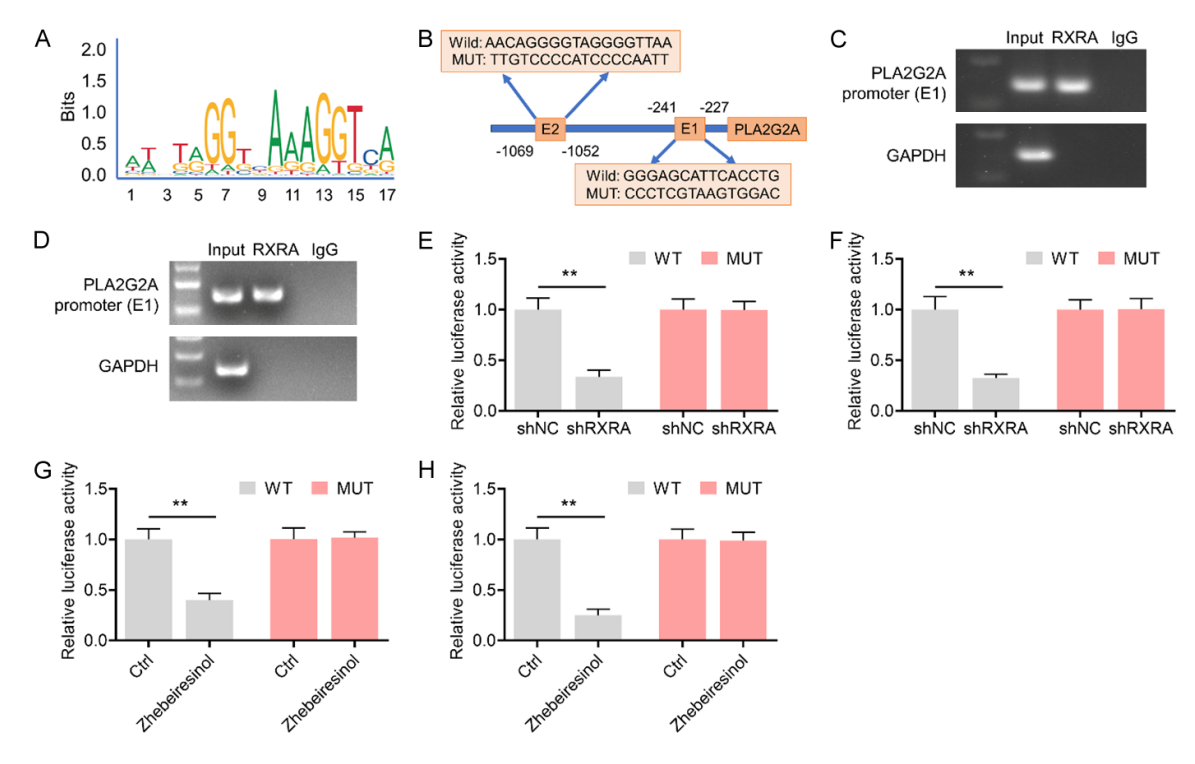


Figure 11. The PLA2G2A mutant failed to bind with RXRA. A. The DNA motif of RXRA was predicted using the JAS-PAR database (http://jaspar.genereg.net/). B. Predicted sites of RXRA binding in the PLA2G2A promoter by gene sequence analysis. C. A ChIP assay was performed to determine the affinity of RXRA for the PLA2G2A promoter E1. D. A ChIP assay was performed to determine the affinity of RXRA for the PLA2G2A promoter E1. E. A dual-luciferase reporter assay was performed by cotransfecting the full-length PLA2G2A promoter or the mutated PLA2G2A promoter (E1 fragment) in 293T cells with the RXRA knockdown plasmid or empty vector. F. A dual-luciferase reporter assay was conducted by cotransfecting the full-length PLA2G2A promoter or the mutated PLA2G2A promoter (E2 fragment) in 293T cells with the RXRA knockdown plasmid or empty vector. G. A dual-luciferase reporter assay was conducted by cotransfecting the full-length PLA2G2A promoter or the mutated PLA2G2A promoter (E1 fragment) in 293T cells with or without zhebeiresinol treatment. H. A dual-luciferase reporter assay was conducted by cotransfecting the full-length PLA2G2A promoter or the mutated PLA2G2A promoter (E2 fragment) in 293T cells with or without zhebeiresinol treatment; **P < 0.01.

damage [31]. The drugs currently used to treat COPD have had limited effects on controlling the progression of COPD. In this study, we found that NLBK significantly inhibited the inflammatory response, mitigated damage to pulmonary function, and improved airway remodeling and ERS in COPD model mice. Next, we determined the composition of zhebeiresinol through network pharmacological analysis and mass spectrometry analysis. The effect target, PLA2G2A, was also determined through bioinformatics analysis. However, rescue experiments revealed that zhebeiresinol had a greater ability to ameliorate the CSE-mediated promotion of the inflammatory response and damage to pulmonary function and to enhance airway remodeling and ERS in COPD model mice. Knocking down PLA2G2A significantly improved the ability of zhebeiresinol to alleviate the symptoms of COPD. Our findings indicated that zhebeiresinol

inhibited the expression of PLA2G2A by suppressing the phosphorylation of RXRA and preventing the entry of RXRA into the nucleus. Additionally, studies on the molecular mechanism revealed that RXRA regulates the transcription of PLA2G2A by binding to its promoter. Our findings suggest that NLBK inhibits the transcription of PLA2G2A by inhibiting the phosphorylation of RXRA and downregulating the expression of RXRA in the nucleus, which inhibits the inflammatory response, ERS, and damage to airway remodeling in mice with COPD. These findings provided a strong scientific basis for treating COPD with traditional Chinese medicine and new ideas for developing new COPD drugs based on traditional Chinese medicine.

Several recent studies have demonstrated that NLBK intervention significantly reduces the

incidence and duration of acute exacerbations of COPD and improves the symptoms of patients with stable COPD [32]. However, the mechanism by which NLBK can alleviate COPD is unclear. Under the effect of infection, smoke. dust, and other factors, neutrophils and macrophages infiltrate the airway, causing the release of TNF-α, IL-6, IL-8, and other inflammatory mediators, leading to the proliferation of goblet cells, hypertrophy of the submucosal glands, an increase in the synthesis of mucin and collagen, and promotion of airway remodeling. We also found that NLBK intervention alleviates the inflammatory reaction caused by CSE, including reducing the levels of TNF- α , IL-1 β , IL-5, IL-10, and IL-13 and increasing the levels of IL-12 and IFN-y. This observation is consistent with our findings in COPD patients [33]. Additionally, our study provides reliable evidence that NLBK intervention partially promotes the effects of CSE on inflammatory cells in the BALF, including total BALF cells, macrophages, eosinophils, neutrophils, CD4+ T lymphocytes, and CD8+ T lymphocytes, providing evidence that NLBK reduces the inflammatory response in COPD patients. Our results also showed that NLBK intervention significantly alleviated lung injury, as indicated by the improvement in lung function, which further confirmed the benefits of NLBK in improving COPD. ERS is a pathogenesis of COPD and is the key signal triggering tissue remodeling under pathological conditions [34]. By investigating ERS-related proteins, we found that NLBK contributed to the reduction in the expression of proteins such as p-PERK, p-IRE1α, ATF4, and ATF6. These findings revealed a new mechanism by which NLBK alleviates COPD and provided a basis for the clinical application of NLBK.

Identifying the downstream targets of NLBK is crucial for determining its molecular mechanism, which may help further elucidate the mechanism underlying the activity of NLBK. In this study, bioinformatics analysis revealed that PLA2G2A was the DEG in COPD patients and was a target of NLBK. PLA2G2A belongs to the phospholipase A2 family and participates in immune regulation and various diseases [35, 36]. Some studies have shown that the expression levels of PLA2G2A in the lung tissue and bronchial secretions of COPD patients may be associated with the severity of the disease

[25]. High expression of PLA2G2A is associated with chronic inflammation and airway remodeling [24, 25]. We found that inhibiting PLA2G2A can protect lung function in a mouse model of COPD [24]. We also found that PLA2G2A was highly expressed in COPD patients. The role of PLA2G2A in COPD and airway inflammation has become an important area of research. Understanding its mechanisms in inflammatory responses and airway remodeling can help in the development of new targeted therapeutic strategies to improve the prognosis of COPD patients.

We identified the active ingredients of NLBK. The results of network pharmacology and mass spectrometry analysis revealed that zhebeiresinol is the active compound of NLBK. The antibacterial activity of zhebeiresinol against Helicobacter pylori was reported in another study [37]. However, whether zhebeiresinol plays a role in reducing inflammation and airway remodeling in COPD mice is not known. Here, we determined the beneficial effects of zhebeiresinol in reducing COPD. The results of the rescue experiments revealed that the effects of zhebeiresinol on reducing COPD are consistent with those of NLBK, including alleviating the inflammatory response and ERS and rescuing airway damage in mice with COPD. By further investigating the relationship between zhebeiresinol and PLA2G2A, we found that zhebeiresinol treatment inhibited the expression of PLA2G2A, and silencing PLA2G2A enhanced the ability of zhebeiresinol to reduce COPD. This included further remission of the inflammatory state, further improvement in lung function, further reduction in ERS-related protein levels, and further improvement in airway recombination-related protein levels. These findings confirmed that the zhebeiresinol/ PLA2G2A axis is needed for NLBK to alleviate COPD, providing a foundation and new regulatory pathways for the clinical application of NLBK in COPD.

Several studies have shown that transcription factors play an important role as a bridge between traditional Chinese medicine prescriptions and targets [38, 39]. A study showed that NLBK exerts beneficial effects on patients with COPD by regulating inflammatory transcription factors, such as nuclear factor kappa-B and activator protein 1 [40, 41]. RXRA was found to

act as a bridge molecule between zhebeiresinol and PLA2G2A. The RXRA/PLA2G2A axis is related to the occurrence and development of COPD [25]. We found that zhebeiresinol and RXRA can directly bind to each other and then prevent the entry of RXRA into the nucleus by inhibiting the phosphorylation of RXRA; this is the first study to identify the downstream targets of zhebeiresinol. This study provided evidence that RXRA can bind to the promoter of PLA2G2A and that RXRA can regulate the transcription of PLA2G2A. This finding is consistent with our findings in the hippocampus of a COPD model of delirium [25]. Our findings suggest that the RXRA/PLA2G2A axis is a new therapeutic target for COPD and provides more effective therapeutic approaches for drug development that target this target, especially for COPD patients who do not respond well to traditional treatments. Zhebeiresinol is a potential therapeutic agent and may offer new treatment options because its mechanism of action involves targeting the RXRA/PLA2G2A axis, especially in alleviating symptoms of COPD and improving lung function.

This study had several limitations. First, we found that zhebeiresinol and RXRA can regulate the transcription of PLA2G2A in COPD, but whether zhebeiresinol directly regulates PLA2G2A needs to be determined. Moreover, seven target genes were also present in COPD and NLBK, and we investigated the mechanisms of these targets. Zhebeiresinol is the active component of NLBK, and zhebeiresinol treatment can rescue damaged lung function in COPD patients. However, whether zhebeiresinol can be used as a single drug to treat COPD and its potential side effects should be carefully considered.

Conclusion

To summarize, we found that NLBK regulates airway remodeling in COPD by inhibiting ERS and the inflammatory response. The active component zhebeiresinol of NLBK inhibits the transcription of PLA2G2A by directly binding and inhibiting the phosphorylation of RXRA, a transcription factor of PLA2G2A. Zhebeiresinol can alleviate CSE-induced airway reorganization by inhibiting PLA2G2A. These results suggested that PLA2G2A-RXRA may be a novel target for COPD and that the therapeutic effects

of zhebeiresinol may not only contribute to a deeper understanding of COPD pathogenesis but also open new avenues for clinical treatment, facilitating the prevention and management of the disease.

Acknowledgements

This study was supported by the Scientific research project supported by the Administration of Traditional Chinese Medicine of Zhejiang province (2024ZR127).

Disclosure of conflict of interest

None.

Address correspondence to: Guodong Wang, Hangzhou TCM Hospital Affiliated to Zhejiang Chinese Medical University, 453 West Round-city Road, Hangzhou 310000, Zhejiang, P. R. China. E-mail: gudowang@163.com

References

- [1] Wang JM, Wang C and Li G. Progress in research of chronic obstructive pulmonary disease and risk factors. Zhonghua Liu Xing Bing Xue Za Zhi 2022; 43: 1343-1348.
- [2] Thomashow BM, Walsh JW and Malanga EDF. The COPD foundation: celebrating a decade of progress and looking ahead to a cure. Chronic Obstr Pulm Dis 2014; 1: 4-16.
- [3] Agustí A, Celli BR, Criner GJ, Halpin D, Anzueto A, Barnes P, Bourbeau J, Han MK, Martinez FJ, Montes de Oca M, Mortimer K, Papi A, Pavord I, Roche N, Salvi S, Sin DD, Singh D, Stockley R, López Varela MV, Wedzicha JA and Vogelmeier CF. Global initiative for chronic obstructive lung disease 2023 report: GOLD executive summary. Eur Respir J 2023; 61: 2300239.
- [4] Janjua S, Mathioudakis AG, Fortescue R, Walker RA, Sharif S, Threapleton CJ and Dias S. Prophylactic antibiotics for adults with chronic obstructive pulmonary disease: a network meta-analysis. Cochrane Database Syst Rev 2021; 1: CD013198.
- [5] Barada O, Salomé-Desnoulez S, Madouri F, Deslée G, Coraux C, Gosset P and Pichavant M. IL-20 cytokines are involved in the repair of airway epithelial barrier: implication in exposure to cigarette smoke and in COPD pathology. Cells 2023; 12: 2464.
- [6] Li W, Li G, Zhou W, Wang H and Zheng Y. Effect of autoimmune cell therapy on immune cell content in patients with COPD: a randomized controlled trial. Comput Math Methods Med 2022; 2022: 8361665.

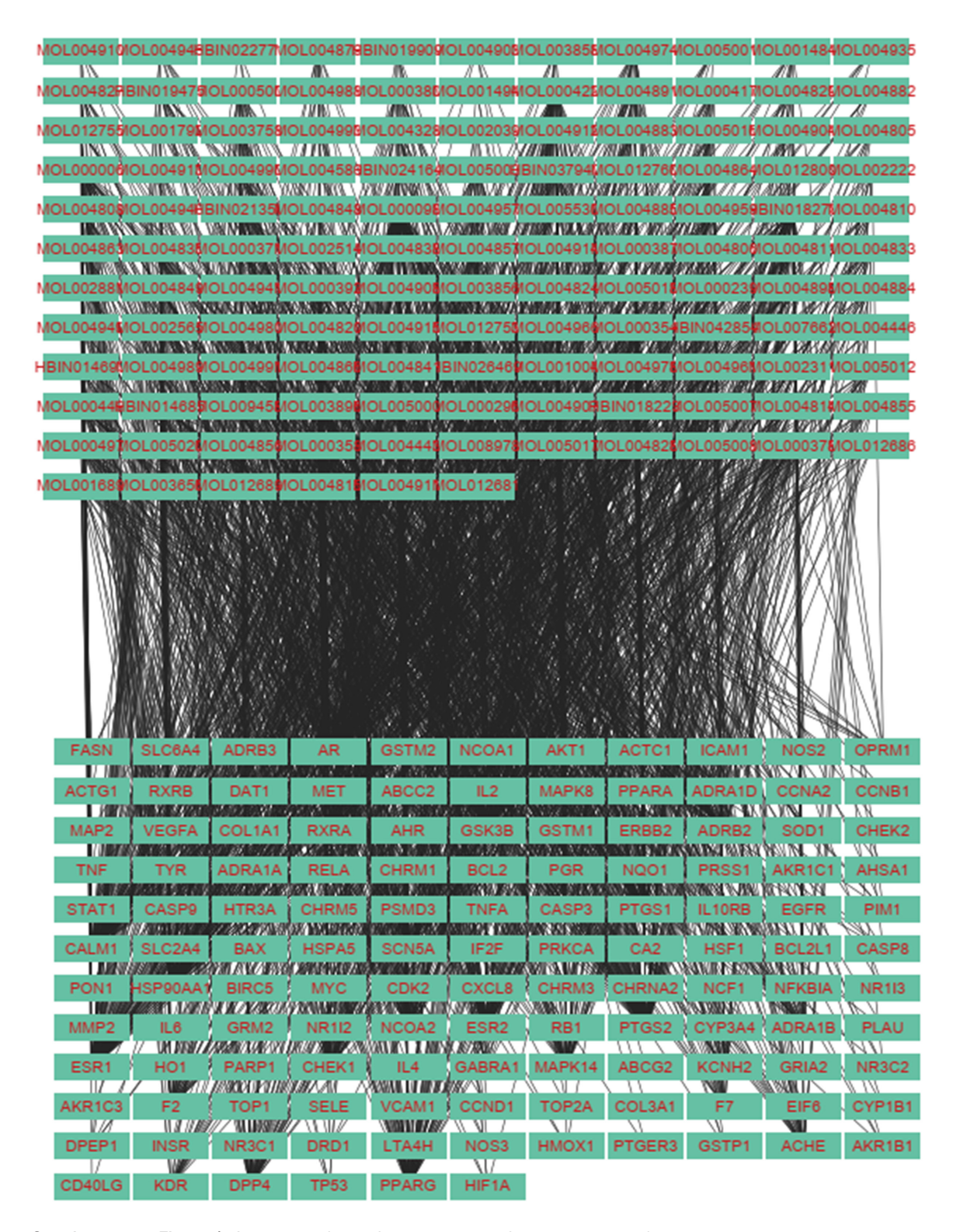
- [7] DI Stefano A, Gnemmi I, Dossena F, Ricciardolo FL, Maniscalco M, Lo Bello F and Balbi B. Pathogenesis of COPD at the cellular and molecular level. Minerva Med 2022; 113: 405-423.
- [8] Zhou P, Yu W, Zhang C, Chen K, Tang W, Li X, Liu Z and Xia Q. Tiao-bu-fei-shen formula promotes downregulation of the caveolin 1-p38 mapk signaling pathway in COPD - associated tracheobronchomalacia cell model. J Ethnopharmacol 2022; 293: 115256.
- [9] Dang K, Ma J, Luo M, Liu Y, Chai Y, Zhu Y, Chen K, Chen J and Liu L. Auricular acupressure as an adjuvant treatment for wheezing in stable chronic obstructive pulmonary disease. J Vis Exp 2024.
- [10] Rabe KF, Martinez FJ, Ferguson GT, Wang C, Singh D, Wedzicha JA, Trivedi R, St Rose E, Ballal S, McLaren J, Darken P, Aurivillius M, Reisner C and Dorinsky P; ETHOS Investigators. Triple inhaled therapy at two glucocorticoid doses in moderate-to-very-severe COPD. N Engl J Med 2020; 383: 35-48.
- [11] Shuai T, Zhang C, Zhang M, Wang Y, Xiong H, Huang Q and Liu J. Low-dose theophylline in addition to ICS therapy in COPD patients: a systematic review and meta-analysis. PLoS One 2021; 16: e0251348.
- [12] Yu XQ, Di JQ, Zhang W, Wei GS, Ma ZP, Wu L, Yu XF, Zhu HZ, Zhou M, Feng CL, Feng JH, Fan P, Li JS and Yang JY. Bu-Fei Yi-Shen granules reduce acute exacerbations in patients with GOLD 3-4 COPD: a randomized controlled trial. Int J Chron Obstruct Pulmon Dis 2023; 18: 2439-2456.
- [13] Li Y, Wang Y, Mao J, Liu X, Wu Z, Bian Q, Li J, Zhang L, Hu Y and Ji H. Bufei Yishen granules decrease inflammation and extracellular matrix deposition in airway remodeling in chronic obstructive pulmonary disease rats. Eur Respir J 2017; 50 Suppl 61: PA1049.
- [14] Lahousse L, Bahmer T, Cuevas-Ocaña S, Flajolet P, Mathioudakis AG, McDonnell M, Uller L, Schleich F, Dortas Junior S, Idzko M, Singh D, Ricciardolo FLM, Adcock IM, Usmani O, Spanevello A and Bonvini SJ. ERS international congress, madrid, 2019: highlights from the airway diseases, asthma and COPD assembly. ERJ Open Res 2020; 6: 00341-2019.
- [15] Duan Q, Zhou Y and Yang D. Endoplasmic reticulum stress in airway hyperresponsiveness. Biomed Pharmacother 2022; 149: 112904.
- [16] Martin R, Nora M, Anna L, Olivia P, Leif B, Gunilla WT, Ellen T and Anna-Karin LC. Altered hypoxia-induced cellular responses and inflammatory profile in lung fibroblasts from COPD patients compared to control subjects. Respir Res 2024; 25: 282.

- [17] Li W, Cao T, Luo C, Cai J, Zhou X, Xiao X and Liu S. Crosstalk between ER stress, NLRP3 inflammasome, and inflammation. Appl Microbiol Biotechnol 2020; 104: 6129-6140.
- [18] Qaisar R, Ustrana S, Muhammad T and Shah I. Sarcopenia in pulmonary diseases is associated with elevated sarcoplasmic reticulum stress and myonuclear disorganization. Histochem Cell Biol 2022; 157: 93-105.
- [19] Zhang X, Liu B, Lal K, Liu H, Tran M, Zhou M, Ezugwu C, Gao X, Dang T, Au ML, Brown E, Wu H and Liao Y. Antioxidant system and endoplasmic reticulum stress in cataracts. Cell Mol Neurobiol 2023; 43: 4041-4058.
- [20] Peng H, Zhou Q, Liu J, Wang Y, Mu K and Zhang L. Endoplasmic reticulum stress: a vital process and potential therapeutic target in chronic obstructive pulmonary disease. Inflamm Res 2023; 72: 1761-1772.
- [21] Kume H, Yamada R, Sato Y and Togawa R. Airway smooth muscle regulated by oxidative stress in COPD. Antioxidants (Basel) 2023; 12: 142.
- [22] Sun R, Jang JH, Lauzon AM and Martin JG. Interferon-gamma amplifies airway smooth muscle-mediated CD4+ T cell recruitment by promoting the secretion of C-X-C-motif chemokine receptor 3 ligands. FASEB J 2021; 35: e21228.
- [23] Mori T, Miyamoto T, Yoshida H, Asakawa M, Kawasumi M, Kobayashi T, Morioka H, Chiba K, Toyama Y and Yoshimura A. IL-1β and TNFαinitiated IL-6-STAT3 pathway is critical in mediating inflammatory cytokines and RANKL expression in inflammatory arthritis. Int Immunol 2011; 23: 701-12.
- [24] Mohammadtursun N, Li Q, Abuduwaki M, Jiang S, Zhang H, Sun J and Dong J. Loki zupa alleviates inflammatory and fibrotic responses in cigarette smoke induced rat model of chronic obstructive pulmonary disease. Chin Med 2020; 15: 92.
- [25] Zhang T and Wang G. Inhibition of RXRA-mediated PLA2G2A improves delirium in COPD mice by regulating endoplasmic reticulum stress pathway and inhibiting cell apoptosis. Cell Mol Biol (Noisy-le-grand) 2024; 70: 226-232
- [26] Jing X, Huo J, Li L, Wang T and Xu J. Baicalin relieves airway inflammation in COPD by inhibiting miR-125a. Appl Biochem Biotechnol 2024; 196: 3374-3386.
- [27] Xiao Y, Zhang J, Shu X, Bai L, Xu W, Wang A, Chen A, Tu WY, Wang J, Zhang K, Luo B and Shen C. Loss of mitochondrial protein CHCHD10 in skeletal muscle causes neuromuscular junction impairment. Hum Mol Genet 2020; 29: 1784-1796.

NLBK alleviates airway remodeling

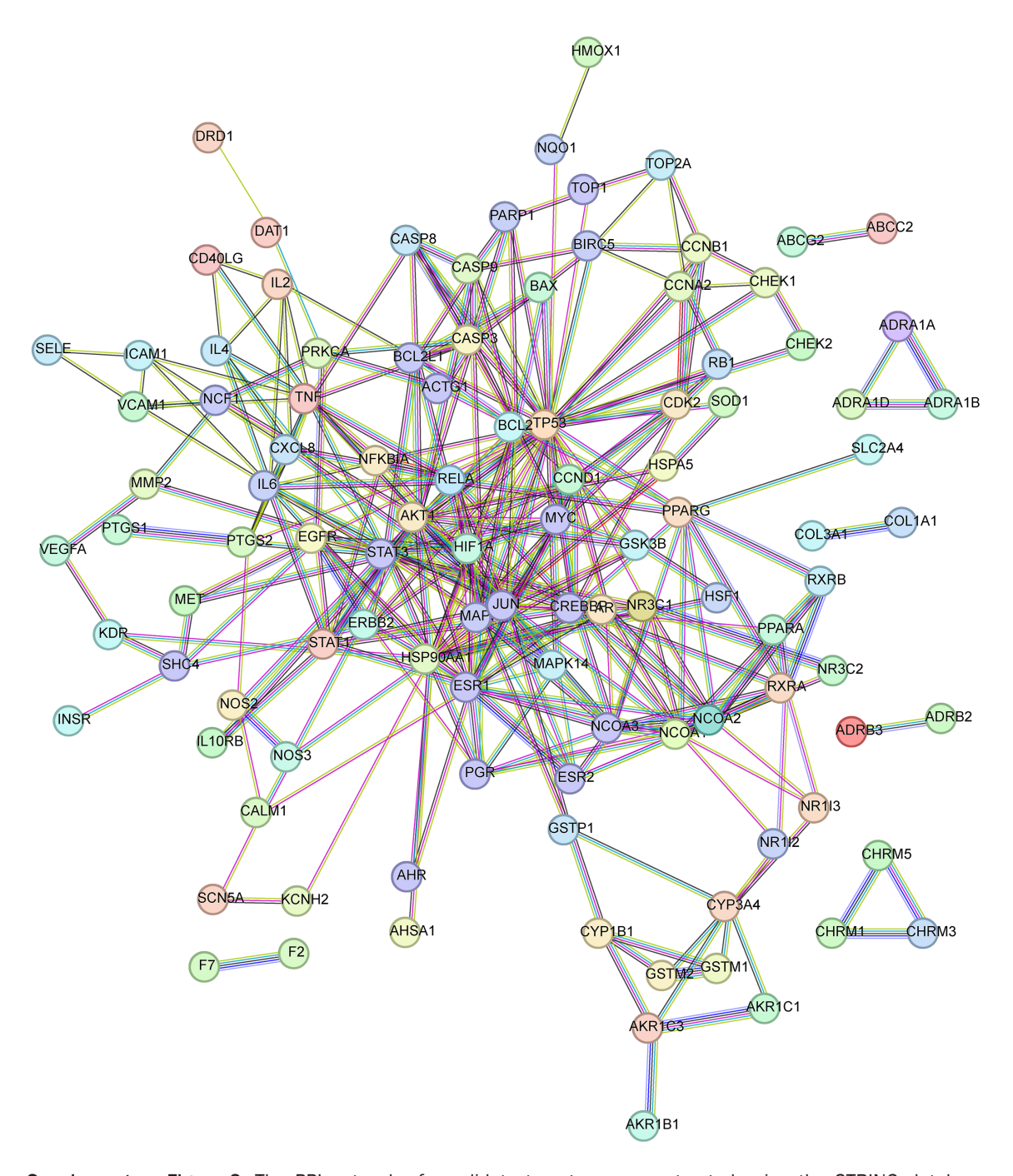
- [28] Wang ZC, Niu KM, Wu YJ, Du KR, Qi LW, Zhou YB and Sun HJ. A dual Keap1 and p47(phox) inhibitor Ginsenoside Rb1 ameliorates high glucose/ox-LDL-induced endothelial cell injury and atherosclerosis. Cell Death Dis 2022; 13: 824.
- [29] Hurst JR, Han MK, Singh B, Sharma S, Kaur G, de Nigris E, Holmgren U and Siddiqui MK. Prognostic risk factors for moderate-to-severe exacerbations in patients with chronic obstructive pulmonary disease: a systematic literature review. Respir Res 2022; 23: 213.
- [30] Dong LL, Liu ZY, Chen KJ, Li ZY, Zhou JS, Shen HH and Chen ZH. The persistent inflammation in COPD: is autoimmunity the core mechanism? Eur Respir Rev 2024; 33: 230137.
- [31] Hulina-Tomašković A, Somborac-Bačura A, Grdić Rajković M, Hlapčić I, Jonker MR, Heijink IH and Rumora L. Extracellular Hsp70 modulates 16HBE cells' inflammatory responses to cigarette smoke and bacterial components lipopolysaccharide and lipoteichoic acid. Cell Stress Chaperones 2022; 27: 587-597.
- [32] Li MY, Qin YQ, Tian YG, Li KC, Oliver BG, Liu XF, Zhao P and Li JS. Effective-component compatibility of Bufei Yishen formula III ameliorated COPD by improving airway epithelial cell senescence by promoting mitophagy via the NRF2/ PINK1 pathway. BMC Pulm Med 2022; 22: 434.
- [33] Li Q, Zhai CM, Zhou J and Ju JF. Clinical study on Yangfei Yishen granules for chronic obstructive pulmonary disease with syndrome of Qi-Yin deficiency in lung and kidney at stable stage. Journal of New Chinese Medicine 2021; 53: 31-35.
- [34] Duan Q, Zhou Y and Yang D. Endoplasmic reticulum stress in airway hyperresponsiveness. Biomed Pharmacother 2022; 149: 112904.

- [35] Ozturk K, Onal MS, Efiloglu O, Nikerel E, Yildirim A and Telci D. Association of 5'UTR polymorphism of secretory phospholipase A2 group IIA (PLA2G2A) gene with prostate cancer metastasis. Gene 2020: 742: 144589.
- [36] Ge W, Yue M, Lin R, Zhou T, Xu H, Wang Y, Mao T, Li S, Wu X, Zhang X, Wang Y, Ma J, Wang Y, Xue S, Shentu D, Cui J and Wang L. PLA2G2A(+) cancer-associated fibroblasts mediate pancreatic cancer immune escape via impeding antitumor immune response of CD8(+) cytotoxic T cells. Cancer Lett 2023; 558: 216095.
- [37] Chen XY, Li JF, Li YS, Yang J, Duan XY, Luo JF, Zhao FW and Wang YH. Chemical constituents from stem bark of Aquilaria sinensis and their antibacterial activity against Helicobacter pylori. Zhongguo Zhong Yao Za Zhi 2024; 49: 4100-4110.
- [38] Yang Z, Zhang Q, Yu L, Zhu J, Cao Y and Gao X. The signaling pathways and targets of traditional Chinese medicine and natural medicine in triple-negative breast cancer. J Ethnopharmacol 2021; 264: 113249.
- [39] Xu X, Wang S, Zhou D, Qu J, Zhang C, Xu Y and Sun L. The Haoqin-Huaban formula alleviates UVB-induced skin damage through HOXA11-AS-mediated stabilization of EZH2. Am J Transl Res 2022; 14: 2212-2230.
- [40] Dong H, Liu X, Zheng W, Feng S, Li J, Qin Y, Wu Y, Chen Y, Yin S and Zhao P. Three Tiaobu Feishen formulae reduces cigarette smoke-induced inflammation in human airway epithelial cells. J Tradit Chin Med 2020; 40: 386-392.
- [41] Li J, Xie Y, Zhao P, Qin Y, Oliver BG, Tian Y, Li S, Wang M and Liu X. A chinese herbal formula ameliorates COPD by inhibiting the inflammatory response via downregulation of p65, JNK, and p38. Phytomedicine 2021; 83: 153475.



Supplementary Figure 1. A compound-putative target network was constructed.

NLBK alleviates airway remodeling



 $\textbf{Supplementary Figure 2.} \ \, \textbf{The PPI network of candidate targets was constructed using the STRING database (https://cn.string-db.org/).}$

Supplementary Files. The results of liquid chromatography-tandem mass spectrometry analysis are presented.